THE ASTROPHYSICAL JOURNAL, 427:483–496, 1994 May 20

EFFECT OF NONLINEAR INTERACTIONS ON *p*-MODE FREQUENCIES AND LINE WIDTHS

PAWAN KUMAR
Department of Physics, Massachusetts Institute of Technology, Cambridge, MA 02139
PETER GOLDREICH
California Institute of Technology, Pasadena, CA 91125
AND
RICHARD KERSWELL
Department of Mathematics, Massachusetts Institute of Technology, Cambridge, MA 02139
Received 1993 June 14; accepted 1993 November 19

ABSTRACT

We calculate the effect of nonlinear interactions among solar acoustic modes upon the modal frequencies and energy loss rates (or line widths). The frequency shift for a radial *p*-mode of frequency 3 mHz is found to be about -0.5 μHz. The magnitude of nonlinear frequency shift increases more rapidly with frequency than the inverse mode mass (mode mass is defined as the ratio of energy in the mode to its surface velocity amplitude squared). This frequency shift is primarily due to nonresonant three-mode interactions and is dominated by high l surface gravity waves (*f*-modes) and *p*-modes. The line width of a radial *p*-mode of frequency 3 mHz, due to resonant nonlinear interactions, is about 0.3 μHz. This result is consistent with that of Kumar & Goldreich (1989). We also find, in agreement with these authors, that the most important nonlinear interactions of trapped *p*-modes involve *f*-modes and high-frequency *p*-modes (frequency greater than about 5 mHz) which propagate in the solar photosphere. Thus, using the arguments advanced by Kumar & Goldreich (1989), we conclude that nonlinear couplings cannot saturate the overstable solar *p*-modes at their small observed amplitudes. Both the nonlinear frequency shifts and line widths, at a fixed frequency, are proportional to the inverse of mode mass which for modes of degree greater than about 100 is $\sim l^{0.8}$. Therefore, the frequency of an *f*-mode of $l = 1000$, due to nonlinear interactions, is decreased by approximately 0.4%.

Subject headings: Sun: oscillations

1. INTRODUCTION

In this paper, we calculate the frequency shifts and energy transfer rates of solar acoustic modes due to nonlinear interactions with other modes. This study is motivated by a desire to assess the importance of such nonlinear interactions in regard to the observed discrepancies between measured and theoretical acoustic mode frequencies (Christensen-Dalsgaard 1991).

This work is a development of an earlier paper by Kumar & Goldreich (1989) (hereafter referred to as KG) who used a planar parallel, adiabatic-plus-isothermal atmosphere to study nonlinear interactions of the solar acoustic modes. Here, we proceed a step further to consider the standard solar model. Following KG, we adopt a Hamiltonian formalism to derive the lowest order nonlinear interactions. This approach is simpler and more elegant than the conventional technique of expanding the equations of motion to second order in wave variables (e.g., Dziembowski 1982; Wentzel 1987; Lavely 1990). The random phase approximation is, as in KG, central to the calculation and we refer the reader there for a discussion. Briefly, the approximation is justified when a large number of oscillators are coupled with approximately the same strength, and typical modal lifetimes are short compared to the nonlinear interaction time, as is the case for the *p*-modes in the Sun.

The paper is organized as follows. In § 2, we describe the Hamiltonian formulation and derive expressions for nonlinear frequency shift and energy transfer rates. Section 3 describes the solar model, the details of the numerical implementation, and contains results concerning frequency shifts and energy drainage rates for radial *p*-modes. Scalings of these quantities for nonradial *p*-modes are also presented here. Section 4 describes a simple model problem which is solved exactly to test our approximate theoretical formula. Finally, our conclusions appear in § 5. The Hamiltonian formalism is outlined in Appendix A, the calculation of coupling coefficients sketched in Appendix B, and a comparison of four-mode couplings to three-mode couplings discussed in Appendix C.

2. FORMULATION

2.1. *Hamiltonian Formalism*

The Hamiltonian of a fluid system is the sum of its kinetic and potential energies (see Appendix A) which we expand in powers of the displacement vector $\boldsymbol{\xi}$. The first-order terms in $\boldsymbol{\xi}$ describe the static equilibrium configuration, the second-order terms yield the linear differential equations which define the normal modes, and the third-order terms describe, in a weakly nonlinear regime, the nonlinear interactions among them. Successive terms describing higher order interactions are neglected under the assumption that the acoustic modes interact only weakly; see Appendix C for justification. The second and third-order parts of the Hamiltonian density appropriate to the adiabatic perturbations of a static configuration composed of an inviscid, compressible gas with variable adiabatic index in a uniform gravitational field take the form (see Appendix A)

$$\mathscr{H} = \mathscr{H}_2 + \mathscr{H}_3 \tag{2.1}$$

with

$$\mathscr{H}_2 = \frac{\rho_0}{2}\left(\frac{\partial \xi}{\partial t}\right)^2 + \frac{1}{2}(\rho_0 c_0^2 - p_0)(\nabla \cdot \xi)^2 + \frac{p_0}{2}\,\xi^i_{;j}\,\xi^j_{;i}\,, \tag{2.2}$$

and

$$\mathscr{H}_3 = -\frac{1}{6}\left[p_0 - \rho_0 c_0^2 + \rho_0^2\left(\frac{\partial c_0^2}{\partial \rho_0}\right)_S\right](\nabla \cdot \xi)^3 + \frac{1}{2}(p_0 - \rho_0 c_0^2)(\nabla \cdot \xi)\xi^i_{;j}\,\xi^j_{;i} + \frac{p_0}{3}\,\xi^i_{;j}\,\xi^j_{;k}\,\xi^k_{;i}\,, \tag{2.3}$$

where p_0, ρ_0 and c_0 are the unperturbed pressure, density, and speed of sound, S is the entropy, $\xi^i_{;j}$ is the covariant derivative of ξ^i with respect to x^j (see Misner, Thorne, & Wheeler 1973 for the definition of covariant derivative), and the summation convention for repeated indices is assumed unless otherwise stated. We expand the displacement vector, ξ, in the terms of normalized displacement eigenvectors, ξ_α, of the system as follows

$$\xi = \sum_\alpha \sqrt{\frac{\omega_\alpha J_\alpha}{2}}\,\{\xi_\alpha(x)\exp(-i\phi_\alpha) + \xi^*_\alpha(x)\exp(+i\phi_\alpha)\}\,, \tag{2.4}$$

where J_α and ϕ_α are action-angle variables, the phase ϕ_α is written in the convenient form $\phi_\alpha(t) = \omega_\alpha t + \epsilon_\alpha$, and the sum over α is a sum over the discrete frequencies of all modes. The eigenfunctions are normalized such that

$$\omega_\alpha^2 \int d^3x \rho \xi_\alpha \cdot \xi^*_\alpha = 1\,. \tag{2.5}$$

Substitution of this normal mode expansion of ξ, equation (2.4), into the second-order Hamiltonian density, equation (2.2), and integration over the volume gives

$$H_2 \equiv \int d^3x\,\mathscr{H}_2 = \sum_\alpha \omega_\alpha J_\alpha = \sum_\alpha E_\alpha \tag{2.6}$$

This represents a series of independent oscillators each with energy $E_\alpha = \omega_\alpha J_\alpha$. Their interaction is described to the lowest order by the third-order Hamiltonian which, after a similar substitution for ξ and integration over space, yields

$$H_3 \equiv \int d^3x\,\mathscr{H}_3 = \sum_{\substack{\alpha,\beta,\gamma \\ s_\alpha, s_\beta, s_\gamma}} \sqrt{\frac{E_\alpha E_\beta E_\gamma}{8}}\,K_{\alpha_{s\alpha}\beta_{s\beta}\gamma_{s\gamma}} \exp\left[-i(s_\alpha\phi_\alpha + s_\beta\phi_\beta + s_\gamma\phi_\gamma)\right]\,, \tag{2.7}$$

where the Greek symbols α, β, γ refer to different modes of oscillation and s_α, s_β, s_γ take the values ± 1. The sum above is over all triplets satisfying the following l and m matching conditions,

$$|l_\beta - l_\gamma| \le l_\alpha \le l_\beta + l_\gamma\,, \qquad s_\alpha m_\alpha + s_\beta m_\beta + s_\gamma m_\gamma = 0\,, \tag{2.8}$$

and the coupling coefficient $K_{\alpha_{s\alpha}\beta_{s\beta}\gamma_{s\gamma}}$ is defined as follows

$$\begin{aligned} K_{\alpha_{s\alpha}\beta_{s\beta}\gamma_{s\gamma}} = -\frac{1}{6}\int d^3x \Bigg\{ & \left[p_0 - \rho_0 c_0^2 + \rho^2\left(\frac{\partial c_0^2}{\partial \rho}\right)_S\right](\nabla \cdot \xi_{\alpha_{s\alpha}})(\nabla \cdot \xi_{\beta_{s\beta}})(\nabla \cdot \xi_{\gamma_{s\gamma}}) \\ & + (\rho_0 c_0^2 - p_0)[(\nabla \cdot \xi_{\alpha_{s\alpha}})\xi^i_{\beta_{s\beta};j}\,\xi^j_{\gamma_{s\gamma};i} + (\nabla \cdot \xi_{\beta_{s\beta}})\xi^i_{\gamma_{s\gamma};j}\,\xi^j_{\alpha_{s\alpha};i} + (\nabla \cdot \xi_{\gamma_{s\gamma}})\xi^i_{\alpha_{s\alpha};j}\,\xi^j_{\beta_{s\beta};i}] + p_0[\xi^i_{\alpha_{s\alpha};j}\,\xi^j_{\beta_{s\beta};k}\,\xi^k_{\gamma_{s\gamma};i} + \xi^i_{\beta_{s\beta};j}\,\xi^j_{\alpha_{s\alpha};k}\,\xi^k_{\gamma_{s\gamma};i}]\Bigg\}\,. \end{aligned} \tag{2.9}$$

In the above expression for $K_{\alpha_{s\alpha}\beta_{s\beta}\gamma_{s\gamma}}$, the complex conjugate eigenfunction is used when $s_\mu = -1$. Note that the coupling coefficient is symmetrical under the interchange of indices $\alpha_{s\alpha}$, $\beta_{s\beta}$, $\gamma_{s\gamma}$. In terms of the action-angle variables, the Hamiltonian is now

$$H = \boldsymbol{\omega} \cdot \boldsymbol{J} + H_3(\boldsymbol{J}, \boldsymbol{\phi})\,, \tag{2.10}$$

where H_3 describes the interactions between oscillators and is considered small compared to $\boldsymbol{\omega} \cdot \boldsymbol{J}$. Hamilton's equations for the time evolution of ϕ's and J's are as follows

$$\frac{d\phi_\alpha}{dt} = \frac{\partial H}{\partial J_\alpha}\,, \tag{2.11}$$

$$\frac{dJ_\alpha}{dt} = -\frac{\partial H}{\partial \phi_\alpha}\,. \tag{2.12}$$

Substituting for H_2 and H_3 from equations (2.6) and (2.7) in the Hamilton's equations, leads to the evolution equations for a given mode α due to its interaction with modes β and γ,

$$\frac{d\phi_\alpha}{dt} = \omega_\alpha + 6\omega_\alpha |K_{\alpha s\alpha\beta s\beta\gamma s\gamma}| \sqrt{\frac{E_\beta E_\gamma}{8E_\alpha}} \cos(\Phi + \delta_3) , \tag{2.13}$$

$$\frac{dJ_\alpha}{dt} = 12 s_\alpha |K_{\alpha s\alpha\beta s\beta\gamma s\gamma}| \sqrt{\frac{E_\alpha E_\beta E_\gamma}{8}} \sin(\Phi + \delta_3) , \tag{2.14}$$

where Φ and δ_3 are defined by

$$\Phi \equiv s_\alpha \phi_\alpha + s_\beta \phi_\beta + s_\gamma \phi_\gamma , \tag{2.15}$$

$$K_{\alpha s\alpha\beta s\beta\gamma s\gamma} = |K_{\alpha s\alpha\beta s\beta\gamma s\gamma}| \exp(-i\delta_3) . \tag{2.16}$$

The combinatorial factors of 6 and 12 in equations (2.13) and (2.14) arise because each triplet (α, β, γ) occurs six times when we sum over all possible modes α, β, and γ in equation (2.7). These two equations form the basis for the study of nonlinear interactions.

2.2. *Frequency Shift and Energy Transfer Rates*

The evolution equations for energy and phase are solved perturbatively by using the expansions:

$$E_\alpha = E_\alpha^{(0)} + E_\alpha^{(1)}(t) + E_\alpha^{(2)}(t) + \cdots , \tag{2.17}$$

$$\phi_\alpha = \epsilon_\alpha + \omega_\alpha t + \phi_\alpha^{(1)}(t) + \phi_\alpha^{(2)}(t) + \cdots , \tag{2.18}$$

where $E_\alpha^{(2)} \ll E_\alpha^{(1)} \ll E_\alpha^{(0)}$ and $\dot{\phi}_\alpha^{(2)} \ll \dot{\phi}_\alpha^{(1)} \ll \omega_\alpha$. Assuming all perturbations are zero at time $t = 0$, we integrate the first-order evolution equations to obtain

$$E_\alpha^{(1)}(t) = 12\omega_\alpha s_\alpha E_\alpha^{(0)} \sum_{\beta,\gamma} \frac{|K_{\alpha s\alpha\beta s\beta\gamma s\gamma}|}{\Delta\omega_{\alpha\beta\gamma}} \sqrt{\frac{E_\beta^{(0)} E_\gamma^{(0)}}{8E_\alpha^{(0)}}} [\cos(\epsilon_3 + \delta_3) - \cos(\Delta\omega_{\alpha\beta\gamma} t + \epsilon_3 + \delta_3)] , \tag{2.19}$$

and

$$\phi_\alpha^{(1)}(t) = 6\omega_\alpha \sum_{\beta,\gamma} \frac{|K_{\alpha s\alpha\beta s\beta\gamma s\gamma}|}{\Delta\omega_{\alpha\beta\gamma}} \sqrt{\frac{E_\beta^{(0)} E_\gamma^{(0)}}{8E_\alpha^{(0)}}} [\sin(\Delta\omega_{\alpha\beta\gamma} t + \epsilon_3 + \delta_3) - \sin(\epsilon_3 + \delta_3)] , \tag{2.20}$$

where

$$\epsilon_3 \equiv s_\alpha \epsilon_\alpha + s_\beta \epsilon_\beta + s_\gamma \epsilon_\gamma , \qquad \Delta\omega_{\alpha\beta\gamma} \equiv s_\alpha \omega_\alpha + s_\beta \omega_\beta + s_\gamma \omega_\gamma .$$

Substituting the above first-order quantities back into the right-hand sides of the evolution equations (2.13) and (2.14), solving for the second-order changes $E_\alpha^{(2)}$ and $\phi_\alpha^{(2)}$, and averaging over the random phases of the modes, leads to

$$\frac{dE_\alpha^{(2)}(t)}{dt} = 9\omega_\alpha \sum_{\beta,\gamma} \frac{|K_{\alpha s\alpha\beta s\beta\gamma s\gamma}|^2 \sin(\Delta\omega_{\alpha\beta\gamma} t)}{\Delta\omega_{\alpha\beta\gamma}} [\omega_\alpha E_\beta^{(0)} E_\gamma^{(0)} s_1 \omega_\beta E_\alpha^{(0)} E_\gamma^{(0)} + s_2 \omega_\gamma E_\beta^{(0)} E_\gamma^{(0)}] , \tag{2.21}$$

$$\frac{d\phi_\alpha^{(2)}(t)}{dt} = -\frac{9\omega_\alpha}{2} \sum_{\beta,\gamma} \frac{|K_{\alpha s\alpha\beta s\beta\gamma s\gamma}|^2}{\Delta\omega_{\alpha\beta\gamma}} [s_\beta \omega_\beta E_\gamma^{(0)} + s_\gamma \omega_\gamma E_\beta^{(0)}][1 - \cos(\Delta\omega_{\alpha\beta\gamma} t)] , \tag{2.22}$$

where

$$s_1 = \frac{s_\beta}{s_\alpha} \quad \text{and} \quad s_2 = \frac{s_\gamma}{s_\alpha} ,$$

The frequency shift of mode α due to nonlinear interactions is $\delta\omega_\alpha \equiv (d\phi_\alpha/dt - \omega_\alpha)$, which to lowest order is given by equation (2.22). The oscillatory term in this equation gives rise to peaks in the power spectrum that are shifted with respect to the main peaks by integer multiples of $\Delta\omega_{\alpha\beta\gamma}$. However, the amplitude of the first sidelobe is smaller compared to the main peak by a factor of $\sim(\delta\omega_\alpha/\Delta\omega_{\alpha\beta\gamma})$, which for nonresonant interactions is a small number (the amplitudes of higher order sidelobes are even smaller). In the next section we show that most of the contribution to $\delta\omega_\alpha$ comes from nonresonant triplets for which $\Delta\omega_{\alpha\beta\gamma} \sim \omega_\alpha$, therefore, the oscillatory term in equation (2.22) can be dropped. The final expression for frequency shift, in this approximation, is given by

$$\delta\omega_\alpha = -\frac{9\omega_\alpha}{2} \sum_{\beta,\gamma} \frac{|K_{\alpha s\alpha\beta s\beta\gamma s\gamma}|^2}{\Delta\omega_{\alpha\beta\gamma}} [s_\beta \omega_\beta \langle E_\gamma \rangle + s_\gamma \omega_\gamma \langle E_\beta \rangle] , \tag{2.23}$$

where the sum over modes β and γ is over all possible triplets, resonant ($\Delta\omega_{\alpha\beta\gamma} \approx 0$) as well as nonresonant, subject only to the constraints of equation (2.8). We see from the above equation that the frequency shift vanishes if only mode α is excited. Moreover, nearly resonant interactions do not contribute much to the frequency shift, in spite of $\Delta\omega_{\alpha\beta\gamma}$ in the denominator, because a triplet can decrease or increase the frequency of mode α, depending on the sign of $\Delta\omega_{\alpha\beta\gamma}$, resulting in the contribution to $\delta\omega_\alpha$ from triplets with $\Delta\omega_{\alpha\beta\gamma} \approx 0$ largely canceling out.

To simplify the expression for the energy transfer rate, we perform the sum over the degree of the second mode, l_β, and without loss of generality choose the difference between the degree of the second and third mode to be δl, i.e., $l_\gamma = l_\beta - \delta l$. The sum over l_β can then be reduced to an integral over $\Delta\omega_{\alpha\beta\gamma}$,

$$\sum_{l_\beta} = \int d\Delta\omega_{\alpha\beta\gamma} \frac{dl_\beta}{d\Delta\omega_{\alpha\beta\gamma}} .$$

Using the dispersion relation for p-modes, $\omega^2 \propto l$, we obtain,

$$\frac{d\Delta\omega_{\alpha\beta\gamma}}{dl_\beta} \approx \frac{1}{2}\left(\frac{s_\beta \omega_\beta}{l_\beta} + \frac{s_\gamma \omega_\gamma}{l_\gamma}\right) \approx \frac{1}{2l_\beta}\left(s_\beta \omega_\beta + s_\gamma \omega_\gamma + \frac{s_\gamma \omega_\gamma \delta l}{l_\beta}\right) .$$

Note that $d\Delta\omega_{\alpha\beta\gamma}/dl_\beta$ is a weak function of $\Delta\omega_{\alpha\beta\gamma}$, and therefore can be taken out of the integral. Its value for resonant triplets ($\Delta\omega_{\alpha\beta\gamma} = 0$) is approximately $-s_\alpha \omega_\alpha/2l_\beta$ (we neglect the $\delta l/l_\beta$ term in the above equation, which is zero for radial oscillations and very small for oscillations with degree less than about 400). Using these results it is easy to derive the following equation,

$$\sum_{l_\beta} \frac{\sin(\Delta\omega_{\alpha\beta\gamma} t)}{\Delta\omega_{\alpha\beta\gamma}} \approx \frac{2\pi l_\beta}{\omega_\alpha} , \tag{2.24}$$

which is used in equation (2.21) to simplify it to the following form

$$\frac{dE_\alpha(t)}{dt} = 36\pi \sum_{l_\gamma, n_\beta, n_\gamma} l_\beta^2 |K_{\alpha s_\alpha \beta s_\beta \gamma s_\gamma}|^2 [\omega_\alpha \langle E_\beta\rangle\langle E_\gamma\rangle + s_1 \omega_\beta \langle E_\gamma\rangle\langle E_\alpha\rangle + s_2 \omega_\gamma \langle E_\alpha\rangle\langle E_\beta\rangle] , \tag{2.25}$$

where the sum is carried out only over resonant triplets ($\Delta\omega_{\alpha\beta\gamma} \approx 0$), which are also subject to the l and m matching conditions described by equation (2.8). One factor of l_β in equation (2.25) comes from summing over m_β, and the other from the integration around resonant peaks (see eq. [2.24]). The physical interpretation of equation (2.25) is simple: mode α gains energy from modes β and γ at a rate proportional to the product of energy in these modes, and loses energy at a rate proportional to the energy in mode α. It can be easily shown that nonlinear interactions drive the system to equipartition.

3. NUMERICAL PROCEDURE AND RESULTS

3.1. *Solar Model and Observational Data*

Our numerical calculations are performed for the solar model of Christensen-Dalsgaard (1991) which extends up to the temperature minimum, upon which an isothermal atmosphere of several scale heights is placed. This added isothermal atmosphere is a crude representation of the optically thin chromosphere, a region above the photosphere whose effect on the nonlinear interactions will be examined. The normal mode calculation for this atmosphere is described in Appendix A. In order to keep mode frequencies above the acoustic cutoff real and thus the eigenfunctions orthogonal, we impose the condition that the Lagrangian pressure perturbation vanishes at the top of the isothermal atmosphere. This leads to a discrete frequency spectrum of both trapped and propagating modes[1] (in KG, a reflecting boundary condition was imposed at infinity to close the system giving rise to a continuous frequency spectrum above the acoustic cutoff frequency). A partial justification for our choice of boundary condition is that the temperature at the top of the solar chromosphere increases by a factor of more than 10 over a short distance, and the density drops by the same factor to maintain pressure equilibrium. This tends to keep the Lagrangian pressure of the layer roughly constant (the situation is analogous to constant air pressure above water in the presence of surface gravity waves). Moreover, mode Coupling strength for all triplets is finite for our atmosphere, whereas KG found that for certain triplets the coupling strength diverges exponentially in the isothermal atmospheres unless truncated at some finite height. Despite these differences, the numerical result for mode line width and frequency shift for the two choices of boundary conditions is found to be nearly the same.

Mode energies are required as input to calculate frequency shift and energy transfer rates (see eqs. [2.23] and [2.25]). Libbrecht & Woodward (1991) have measured surface velocities of low-degree ($l \leq 50$), solar p-modes in the 5 minute band. However, mode energies are poorly known for high degree modes which make most of the contribution to mode couplings. Therefore, we have carried out numerical calculations for two different choices of high-degree modal energies; one of which is to assume that the surface velocity amplitude of p-modes is l-independent (at fixed frequency) for $l > 200$, and mode energies are l-independent below l of 200. The other prescription we use is to take the surface velocity amplitude from Kaufman (1991), who has measured the power spectrum of solar modes of degree up to 700 and finds that mode velocities are decreasing with l. In fact we use a crude fit to Kaufman's power spectrum for numerical computations; the surface velocity squared of modes is taken to be proportional to $1/l$ for $l > 200$, and as in the other model the mode energies are assumed to be l-independent below 200.

3.2. *Outline of Numerical Scheme*

The equations of adiabatic, nonradial oscillations (eqs. [A12] and [A13]) are solved for the boundary conditions given in Appendix A using a shooting method. Numerical calculations for frequency shifts and energy transfer rates have been carried out only for radial modes. We present an approximate scaling for nonradial modes in § 3.5. The frequency shift is evaluated by carrying out the sum in equation (2.23) over all possible mode triplets that satisfy the l and m matching conditions ($l_\beta = l_\gamma$, and $s_\beta m_\beta + s_\gamma m_\gamma = 0$).

[1] Propagating is used to refer to modes which are oscillatory in the isothermal atmosphere as opposed to trapped modes which are evanescent.

Mode triplets are obtained by choosing the second mode β to lie along different ridges in the l-ν diagram (mode α is the first mode). From the l selection rule we know that the third mode (γ) must have the same l-value as mode β, and therefore all possible γ's are obtained by varying n_γ from 0 to some maximum value. In fact both the coupling coefficient and the mode energies fall off rapidly with increasing n_β and n_γ. Therefore we sum over only the first five ridges in the l-ν diagram.

The computation of energy transfer rates due to nonlinear interactions involves a similar summation procedure of equation (2.25) over all resonant triplets. The resonant triplets are found by shifting each ridge in the l-ν diagram vertically by an amount equal to ω_α (the frequency of the mode of interest), and determining its intersection with all other ridges.

3.3. *Order of Magnitude Estimate*

In this subsection, we provide an order of magnitude estimate for the nonlinear frequency shift and line width. This will give physical insight into the results of the numerical calculation presented in the next subsection, which might otherwise appear somewhat obscure.

We begin by estimating the magnitude of the coupling coefficient $K_{\alpha\beta\gamma}$. Using the constancy of the acoustic energy flux in the wave propagation region, we find that the displacement eigenfunction for p-modes is proportional to $1/(\rho c)^{1/2}$. The displacement eigenfunction for f-modes, on the other hand, decreases exponentially with depth. The three-mode coupling coefficient (see eq. [2.9]) can be approximated by $K_{\alpha\beta\gamma} \sim R_\odot^2 \int dr\, p\xi_\alpha \xi_\beta \xi_\gamma k_\alpha k_\beta k_\gamma$, where the k's are wavenumbers which take values $\sim\omega^2/g$ in the photosphere (here the waves are evanescent), and ω/c in the region where waves are oscillating (see Goldreich & Kumar 1990). Making use of the scaling properties of the ξ's and k's in the above expression for $K_{\alpha\beta\gamma}$ we find that the integrand decreases rapidly with depth, and therefore most of the contribution to the three-mode coupling coefficient comes from a region close to the photosphere. Thus in evaluating the integral, we can use the value of the displacement eigenfunction at the surface, which is given by $1/(\omega \mathcal{M}^{1/2})$, where $\mathcal{M}$ is the mode mass defined as the ratio of energy in the mode to its surface velocity amplitude squared. The coupling coefficient is now easily estimated to be $l_\beta R_\odot p_s H_s \omega_\alpha/[g^2(\mathcal{M}_\alpha \mathcal{M}_\beta \mathcal{M}_\gamma)^{1/2}]$; where p_s and H_s are photospheric gas pressure and scale height, and g is the gravitational acceleration. In arriving at the above result, we have assumed that mode α is a low-degree mode, that β and γ are high-degree modes, and that the dispersion relation for high-degree modes is $\omega^2 \approx gl/R_\odot$. The typical mode mass for high-degree modes can be easily estimated from the scaling property of ξ derived above. Briefly, the total energy in a mode is $\omega^2 \int d^3x \rho \xi^2 \sim \omega^2 \rho_s c_s R_\odot^2 \xi_s^2 \int dr/c$ (the subscript s here refers to the photospheric value). The above integral is equal to the sound travel time across the cavity in which the mode is trapped, which is roughly equal to π/ω. Thus the mode mass is approximately equal to $\pi R_\odot^2 \rho_s c_s/\omega$, or a few times 10^{23}. Substituting this in the above derived expression for the coupling coefficient, we find that $K_{\alpha\beta\gamma}$ is $\sim 10^{-19}$ for $l_\beta = 2000$.

The energy spectrum of solar oscillations of a fixed degree is well known to peak at about 3 mHz (Libbrecht & Woodward 1991) and is only weakly dependent on mode degree. Furthermore, as shown above, the three-mode coupling coefficients increase with degree (and thus frequency) of modes β and γ. Due to these two opposing effects, most of the contribution to the nonlinear frequency shift and line width comes from those triplets which have modes β and γ lying on the first few ridges in the l-ν diagram between degrees of approximately 1000 and 2000. We now have all the ingredients needed to estimate modal line width and frequency shift due to nonlinear interactions.

From equation (2.25) we find that $d(\ln E_\alpha)/dt \sim 36\pi N_{\rm rt} |K_{\alpha\beta\gamma}|^2 E_\beta l_\beta^2 \omega_\beta$. Here $N_{\rm rt}$ is the number of resonant triplets which have different values for n_β and n_γ (on the order of 10 for radial p-modes), and E_β is the typical energy of high degree modes $\sim 10^{23}$ ergs. Thus the modal line width due to nonlinear interactions is ~ 0.1 μHz, or about a factor of 10 smaller than the observed line width.

We use equation (2.23) to estimate the change in the eigenfrequency of p-modes due to nonlinear interactions. Due to the factor $\Delta\omega_{\alpha\beta\gamma}$ in the denominator (eq. [2.23]) the contributions from resonant triplets nearly cancel, and so in estimating frequency shift we will consider nonresonant interactions. The total number of nonresonant triplets for the degree of the second mode less than or equal to l_β is $4N_{\rm rt} l_\beta^2$; and the typical value of $\Delta\omega_{\alpha\beta\gamma}$ for these triplets is $\sim\omega_\alpha$. Putting it all together, we find that $\delta\omega_\alpha \sim 18 N_{\rm rt} \omega_\beta E_\beta l_\beta^2 |K_{\alpha\beta\gamma}|^2$ or 0.02 μHz (this is smaller than the numerical calculation by about a factor of 10).

3.4. *Results*

Table 1 displays the frequency shift and modal line width generated by nonlinear interactions with other p-modes for the case where the surface velocities of modes of degree greater than 200 are assumed to be l-independent. Table 2 shows the same quantities for the other choice of p-mode energy spectrum when mode velocities at the surface are assumed to be proportional to $1/l^{1/2}$ for $l > 200$. Both the frequency shift, $\delta\omega_{\rm 3mc}$,[2] and the line width, $\Gamma_{\rm 3mc}$, are rapidly increasing functions of mode frequency; at 3 mHz the frequency shift is about -0.5 μHz, and line width is about 0.4 μHz. In Figure 1 we plot $\mathcal{M}\delta\omega_{\rm 3mc}$ (where $\mathcal{M}$ is mode mass, which is defined as the ratio of energy in the mode to its surface velocity amplitude squared) and $\mathcal{M}\Gamma_{\rm 3mc}$ as a function of mode frequency ω. Note that both $|\delta\omega_{\rm 3mc}|$, and $\Gamma_{\rm 3mc}$ are increasing more rapidly with frequency than the inverse mode mass. Nonlinear mode line width, $\Gamma_{\rm 3mc}$, starts to decline at high frequencies when the gain of energy from lower frequency modes starts to compete with the energy loss to higher frequency waves.

Figure 2 shows the contribution to $\delta\omega_{\rm 3mc}$ as a function of triplet frequency mismatch, $\Delta\omega_{\alpha\beta\gamma}$, for two different radial p-modes. The dominant feature, common to all modes, is the large antisymmetric peaks around $\Delta\omega_{\alpha\beta\gamma} = 0$. This arises due to nearly resonant triplets for which $\Delta\omega_{\alpha\beta\gamma} \approx 0$ and thus the denominators in equation (2.23) become small. These near-resonant triplets, however, make negligible contribution to $\delta\omega_{\rm 3mc}$ because of the large cancellation due to the antisymmetric peaks. To illustrate this point more clearly we have integrated the curves in Figure 2 from $-\Delta\omega_{\alpha\beta\gamma}$ to $\Delta\omega_{\alpha\beta\gamma}$ and plotted the resultant integrated contribution to $\delta\omega_{\rm 3mc}$ as a function of $\Delta\omega_{\alpha\beta\gamma}$ in Figure 2 (*dashed line*). Note that triplets with $|\Delta\omega_{\alpha\beta\gamma}| \geq 1$ mHz make most of the contribution to the nonlinear frequency shift. This result justifies neglecting the oscillatory terms in equation (2.22).

[2] 3mc = 3 mode coupling.

TABLE 1

FREQUENCY SHIFT AND LINE WIDTHS OF RADIAL p-MODES DUE TO NONLINEAR INTERACTIONS

		$\delta\nu_\alpha$ (μHz)		$\Gamma_{\alpha,3mc}$ (μHz)	
ν_α (mHz)	E_α (ergs)	$h = 0\ H_p$	$h = 5.0\ H_p$	$h = 0\ H_p$	$h = 5.0\ H_p$
1.016.....	0.427E+27	+0.186E−4	−0.502E−4	0.225E−3	0.261E−3
1.300.....	0.427E+27	−0.249E−3	−0.525E−3	0.346E−3	0.421E−3
1.577.....	0.427E+27	−0.377E−2	−0.293E−2	0.405E−2	0.414E−2
1.846.....	0.592E+27	−0.167E−1	−0.253E−1	0.112E−1	0.101E−1
2.116.....	0.796E+27	−0.604E−1	−0.605E−1	0.423E−1	0.282E−1
2.382.....	0.134E+28	−0.158E+0	−0.167E+0	0.110E+0	0.879E−1
2.649.....	0.245E+28	−0.343E+0	−0.320E+0	0.248E+0	0.157E+0
2.919.....	0.393E+28	−0.442E+0	−0.532E+0	0.399E+0	0.211E+0
3.189.....	0.501E+28	−0.588E+0	−0.796E+0	0.611E+0	0.304E+0
3.461.....	0.263E+28	−0.869E+0	−0.112E+1	0.831E+0	0.316E+0
3.734.....	0.110E+28	−0.126E+1	−0.138E+1	0.102E+1	0.349E+0
4.008.....	0.515E+27	−0.129E+1	−0.171E+1	0.131E+1	0.320E+0
4.284.....	0.305E+27	−0.158E+1	−0.214E+1	0.159E+1	0.332E+0
4.559.....	0.174E+27	−0.182E+1	−0.269E+1	0.190E+1	0.349E+0
4.836.....	0.951E+26	−0.209E+1	−0.348E+1	0.208E+1	0.508E+0
5.113.....	0.531E+26	−0.239E+1	−0.457E+1	0.142E+1	0.290E+0

NOTE.—Frequency shift ($\delta\nu_\alpha \equiv \delta\omega_\alpha/2\pi$) and mode line width, $\Gamma_{\alpha,3mc} \equiv -d\ln E_\alpha/dt$, for radial acoustic modes due to nonlinear interactions. The mode frequencies and their shifts given in this table are cyclic frequencies. We denote by h the thickness of the isothermal atmosphere, which is placed above the temperature minimum, in units of the pressure scale height H_p. The results in this table are calculated with mode energies independent of l (at fixed frequency) for l less than 200, and declining at high l such that the surface velocity is l-independent.

Other prominent features in Figure 2 are the presence of large contributions at $\omega_\alpha \pm 6$ mHz and a "quiet zone" (which makes no contribution to frequency shift) centered at $\Delta\omega_{\alpha\beta\gamma} = \omega_\alpha$ and bordered by an antisymmetric spike. The first feature is a manifestation of the energy peak at 3 mHz in the acoustic modes. At $\Delta\omega_{\alpha\beta\gamma} = \omega_\alpha \pm (\omega_\beta - \omega_\gamma)$ the contribution is small because the two terms in equation (2.23) have opposite sign, whereas at $\Delta\omega_{\alpha\beta\gamma} = \omega_\alpha \pm (\omega_\beta + \omega_\gamma)$ the two terms have the same sign and so we obtain the large contribution observed. The height of these peaks is approximately proportional to $1/\Delta\omega_{\alpha\beta\gamma}$. Therefore, as ω_α increases, the height of peak at $\Delta\omega_{\alpha\beta\gamma} = \omega_\alpha + 6$ mHz becomes smaller, and that at $\Delta\omega_{\alpha\beta\gamma} = \omega_\alpha - 6$ mHz increases (see Fig. 2). The "quiet zone" arises due to two reasons. First, since mode α is radial, $l_\beta = l_\gamma$, and so the minimum value of $|\omega_\beta - \omega_\gamma|$ is the minimum spacing between

TABLE 2

FREQUENCY SHIFT AND LINE WIDTHS OF RADIAL p-MODES DUE TO NONLINEAR INTERACTIONS

		$\delta\nu_\alpha$ (μHz)		$\Gamma_{\alpha,3mc}$ (μHz)	
ν_α (mHz)	E_α (ergs)	$h = 0\ H_p$	$h = 5.0\ H_p$	$h = 0\ H_p$	$h = 5.0\ H_p$
1.016.....	0.427E+27	−0.117E−4	−0.226E−4	0.363E−4	0.415E−4
1.300.....	0.427E+27	−0.201E−3	−0.222E−3	0.797E−4	0.773E−4
1.577.....	0.427E+27	−0.158E−2	−0.142E−2	0.838E−3	0.781E−3
1.846.....	0.592E+27	−0.698E−2	−0.831E−2	0.239E−2	0.195E−2
2.116.....	0.796E+27	−0.223E−1	−0.228E−1	0.990E−2	0.623E−2
2.382.....	0.134E+28	−0.575E−1	−0.590E−1	0.280E−1	0.183E−1
2.649.....	0.245E+28	−0.113E+0	−0.109E+0	0.637E−1	0.338E−1
2.919.....	0.393E+28	−0.151E+0	−0.172E+0	0.103E+0	0.485E−1
3.189.....	0.501E+28	−0.202E+0	−0.246E+0	0.160E+0	0.710E−1
3.461.....	0.263E+28	−0.278E+0	−0.322E+0	0.216E+0	0.763E−1
3.734.....	0.110E+28	−0.355E+0	−0.386E+0	0.272E+0	0.876E−1
4.008.....	0.515E+27	−0.380E+0	−0.457E+0	0.341E+0	0.827E−1
4.284.....	0.305E+27	−0.433E+0	−0.540E+0	0.409E+0	0.817E−1
4.559.....	0.174E+27	−0.481E+0	−0.639E+0	0.489E+0	0.788E−1
4.836.....	0.951E+26	−0.534E+0	−0.774E+0	0.544E+0	0.873E−1
5.113.....	0.531E+26	−0.579E+0	−0.943E+0	0.464E+0	0.300E−1

NOTE.—Frequency shift ($\delta\nu_\alpha \equiv \delta\omega_\alpha/2\pi$) and mode line width, $\Gamma_{\alpha,3mc} \equiv -d\ln E_\alpha/dt$, for radial acoustic modes due to nonlinear interactions. The mode frequencies and their shifts given in this table are cyclic frequencies. We denote by h the thickness of the isothermal atmosphere, which is placed above the temperature minimum, in units of the pressure scale height H_p. Results in this table are calculated with mode energies independent of their degree (at fixed frequency) for l less than 200, and at higher degrees the surface velocity squared is taken to be decreasing linearly with l as has been suggested by the observations of Kaufman (1991).

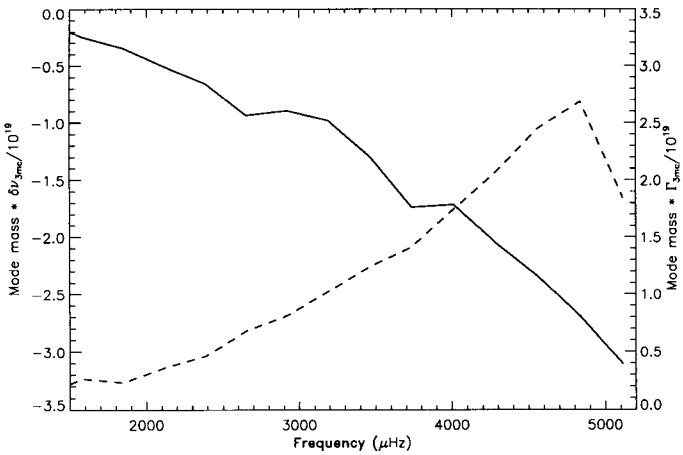

FIG. 1.—Plot of $\mathcal{M}\delta\nu_{3mc}$ (*solid line*), and $\mathcal{M}\Gamma_{3mc}$ (*dashed line*) for radial modes as a function of frequency. Mode mass, $\mathcal{M}$, decreases rapidly with frequency below ~3 mHz ($\mathcal{M} \propto \nu^{-5}$), and remains roughly constant above it. The turnover in Γ_{3mc} occurs when energy gain from lower frequency modes becomes comparable to the energy loss to propagating acoustic waves.

adjacent ridges in the l-ν plane (it is easy to see from eq. [2.23] that those triplets for which $\omega_\beta = \omega_\gamma$, and $s_2/s_1 = -1$ do not contribute to the frequency shift) giving arise to a region around $\Delta\omega_{\alpha\beta\gamma} = \omega_\alpha$ which does not contribute to $\delta\omega_\alpha$. Second, we have chosen a minimum value of ω_β as 0.5 mHz (because coupling coefficients are small at low frequencies, see Fig. 3). Therefore, the minimum value of $\omega_\beta + \omega_\gamma$ is 1.0 mHz giving rise to a gap of size 2.0 mHz. It is the smaller of these two gaps which appears in our plots.

Frequency shifts are not very sensitive to the thickness of the isothermal atmosphere placed on top of the solar model at the temperature minimum, whereas line widths at 3 mHz vary by a factor of 2 for the two cases we have considered (see Table 1 and 2). The reason for this difference is that a significant contribution to nonlinear frequency shifts comes from couplings to trapped modes which are evanescent in the isothermal atmosphere and therefore their eigenfunctions do not grow very much with height. By contrast, nonlinear mode line widths are dominated by those triplets which contain one propagating mode (see KG for detailed discussion) whose eigenfunction is increasing as $1/(\rho c)^{1/2}$, and therefore coupling coefficients and consequently line widths are sensitive to the thickness of the isothermal atmosphere.

In Figure 3 we show the three-mode coupling coefficient, $K_{\alpha\beta\gamma}$, as a function of l_β, n_β, and n_γ for a mode of frequency 3.7 mHz. For small values of ω_α, the coupling coefficients are largest when both modes β and γ are on the same ridge. As mode γ moves away onto neighboring ridges, the coefficient quickly decreases. This behavior, however, is less pronounced when ω_α is close to 5 mHz. The largest three-mode couplings, for any mode, are with modes lying on the lowest or zeroth ridge; the coupling coefficients involving modes lying on the third ridge ($n = 3$) are typically smaller compared to with f-modes ($n = 0$) by a factor of about 5.

We find that the values of the line widths due to nonlinear interactions are quite similar to the results obtained by KG. Moreover, the contribution is dominated by the f-modes and falls off rapidly with increasing ridge number in agreement with KG (see Fig. 4). Thus the arguments suggested by these authors, based on plane parallel adiabatic-plus-isothermal atmosphere approximation to the solar structure, as to why the amplitudes of p-modes can not be saturated by nonlinear couplings at the observed amplitude applies to p-modes in the Sun.

3.5. *Frequency Shift and Energy Transfer Rates for Nonradial Oscillations*

We have so far calculated frequency shifts and energy drainage rates for radial acoustic modes only. We now estimate the magnitude of these quantities for nonradial p-modes. The degree of mode α (l_α) enters our calculations in two places. In the first place it increases the phase space of allowed triplets, and in the second it modifies $K_{\alpha\beta\gamma}$. The first effect is straightforward to calculate. There are more contributing triplets for nonradial oscillations, since the condition, $l_\beta = l_\gamma$, for radial mode is replaced by the triangularity condition, $|l_\beta - l_\alpha| \leq l_\gamma \leq l_\beta + l_\alpha$, for a nonradial oscillation; thus the phase space of mode triplets is larger by a factor $(2l_\alpha + 1)$.

The dependence of $K_{\alpha\beta\gamma}$ on l_α comes from both the angular and the radial part of eigenfunctions. When mode α is radial, the angle dependent integrand of the three-mode coupling coefficient is a product of two spherical harmonic functions, and thus evaluates trivially to 1. In the general case, however, the angular integral is product of three spherical harmonic functions which we denote by Z defined below,

$$\int d\Omega Y_{l_\alpha}^{m_\alpha} Y_{l_\beta}^{m_\beta} Y_{l_\gamma}^{m_\gamma} \equiv Z_{m_\alpha m_\beta m_\gamma}^{l_\alpha l_\beta l_\gamma} .$$

Using the notation and results from Edmonds (1960) we can express the function Z in the terms of Wigner 3-j symbols as follows:

$$Z_{m_\alpha m_\beta m_\gamma}^{l_\alpha l_\beta l_\gamma} = \sqrt{\frac{(2l_\alpha + 1)(2l_\beta + 1)(2l_\gamma + 1)}{4\pi}} \begin{pmatrix} l_\alpha & l_\beta & l_\gamma \\ 0 & 0 & 0 \end{pmatrix} \begin{pmatrix} l_\alpha & l_\beta & l_\gamma \\ m_\alpha & m_\beta & m_\gamma \end{pmatrix} .$$

This is equation (4.6.3) of Edmonds. To carry out the sum over m_β and m_γ in the expressions for energy loss rates and frequency shifts for mode α (see eqs. [2.21] and [2.23]) we only need to focus on Z^2, because mode energies, line widths, eigenfrequencies, and the

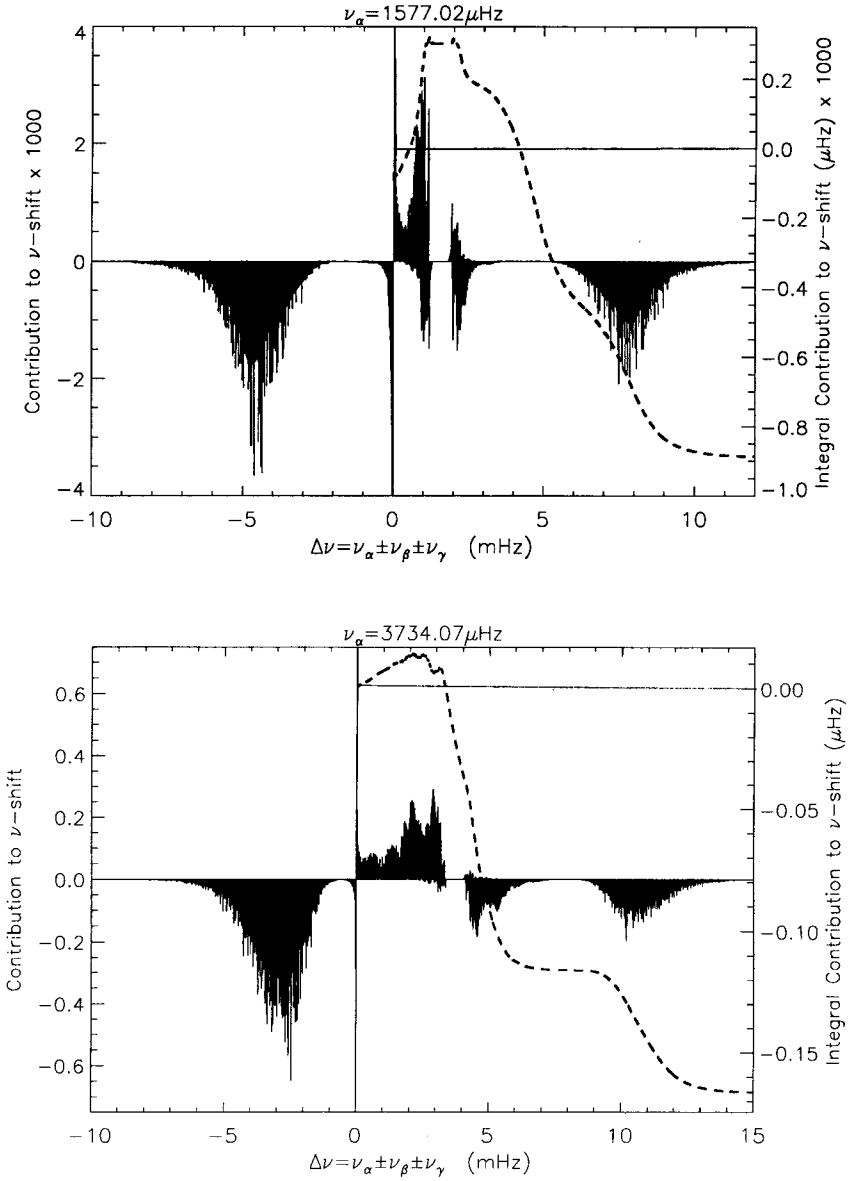

FIG. 2.—(*a*) Contribution to nonlinear frequency shift for a radial *p*-mode of frequency 1577.02 μHz as a function of triplet frequency mismatch $\Delta\omega_{\alpha\beta\gamma}$ (*black areas*). The velocity power spectrum of high-degree modes, for this calculation, was taken to be $\propto 1/l$ above l of 200. The different features of this curve are explained in the text. The dashed curve is obtained by integrating the differential contribution (*black area*) from $-\delta\nu$ to $+\delta\nu$, which is useful for determining the contribution to frequency shift from all triplets with $|\Delta\omega_{\alpha\beta\gamma}| < \delta\nu$. It clearly shows that the frequency shifts are caused by nonresonant couplings for which $|\Delta\omega_{\alpha\beta\gamma}| \sim \omega_\alpha$. (*b*) Same as (*a*), except that the frequency of the radial mode here is 3734.1 μHz.

radially dependent eigenfunction are all m independent for the nonrotating Sun considered here. The sum of Z^2 over m_β and m_γ is easily carried out using the following identity due to Edmonds (his eq. [3.7.8]):

$$\sum_{m_\beta, m_\gamma} \begin{pmatrix} l_\alpha & l_\beta & l_\gamma \\ m_\alpha & m_\beta & m_\gamma \end{pmatrix} \begin{pmatrix} l_\alpha & l_\beta & l_\gamma \\ m_\alpha & m_\beta & m_\gamma \end{pmatrix} = (2l_\alpha + 1)^{-1}\delta(l_\alpha l_\beta l_\gamma) ,$$

where $\delta(l_\alpha l_\beta l_\gamma)$ is defined to be 1 if l_α, l_β, and l_γ satisfy the triangularity condition or otherwise it is 0. This leads to

$$\sum_{m_\beta, m_\gamma} |Z^{l_\alpha l_\beta l_\gamma}_{m_\alpha m_\beta m_\gamma}|^2 = \frac{(2l_\beta + 1)(2l_\gamma + 1)}{4\pi} \begin{pmatrix} l_\alpha & l_\beta & l_\gamma \\ 0 & 0 & 0 \end{pmatrix}^2 .$$

We can simplify this expression by making use of equation (3.7.17) of Edmonds for the 3-*j* symbol appearing in the above equation

$$\begin{pmatrix} l_\alpha & l_\beta & l_\gamma \\ 0 & 0 & 0 \end{pmatrix} = \sqrt{\frac{(l_\alpha + l_\beta - l_\gamma)!(l_\alpha + l_\gamma - l_\beta)!(l_\beta + l_\gamma - l_\alpha)!}{(l_\alpha + l_\beta + l_\gamma + 1)!}} \frac{[(l_\alpha + l_\beta + l_\gamma)/2]!}{[(l_\beta + l_\gamma - l_\alpha)/2]![(l_\alpha + l_\gamma - l_\beta)/2]![(l_\alpha + l_\beta - l_\gamma)/2]!} .$$

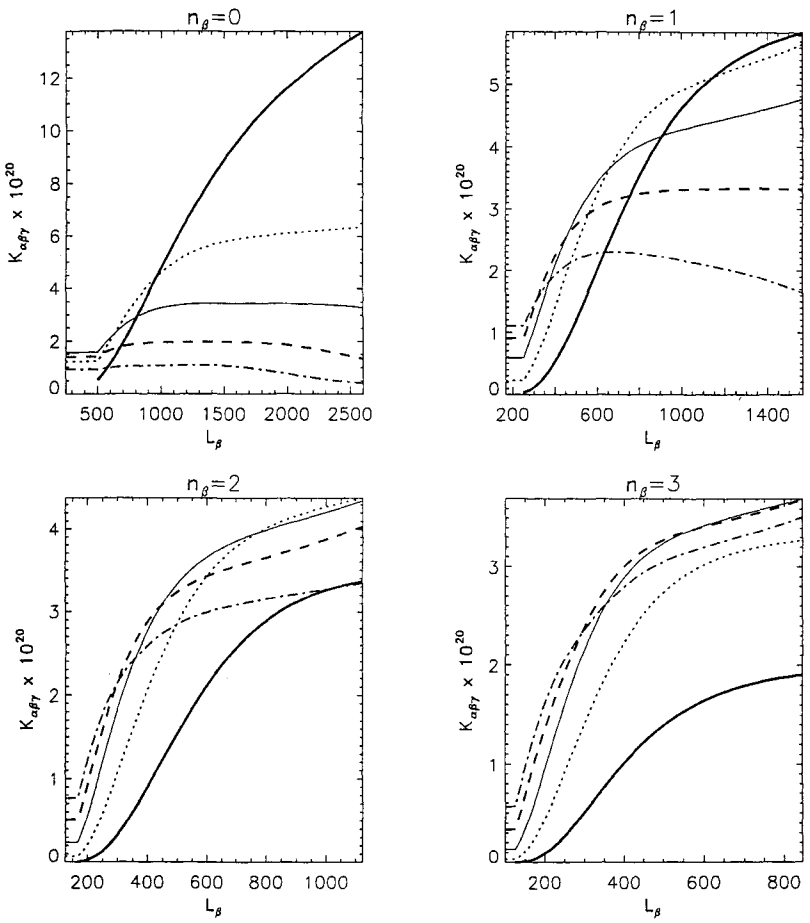

FIG. 3.—Plots of coupling coefficients as a function of the degree of the second mode (l_β); the frequency of mode α is 3734.1 μHz. The four panels correspond to the second mode lying on four different ridges (n_β) which are indicated in the heading of each panel. The five different curves in each panel correspond to different values for n_γ (the ridge number of the third mode of the triplet). These values are: $n_\gamma = 0$ (*thick solid curve*), $n_\gamma = 1$ (*dotted curve*), $n_\gamma = 2$ (*thin solid curve*), $n_\gamma = 3$ (*dashed curve*), and $n_\gamma = 4$ (*dash-dot curve*). The main features to note here are that the coupling coefficient ($K_{\alpha\beta\gamma}$) in general increases with increasing l_β, it decreases with n_β, and that typically $K_{\alpha\beta\gamma}$ is largest when modes β and γ lie on the same ridge and decreases with increasing $|n_\beta - n_\gamma|$.

Applying Stirling's approximate formula for evaluating factorials (or evaluating the above expression numerically), we find that the sum of Z^2 over m_β is proportional to $1/l_\alpha$. As a result, a typical coupling term for nonradial oscillations is reduced by a factor of $1/l_\alpha$ compared to the radial case. However, as we have seen above, the phase space is larger for nonradial modes by a factor of l_α which balances the weakened individual interactions. Therefore, the dependence of frequency shift and line width on l_α comes only through the radial dependence of the displacement eigenfunction.

The surface displacement amplitude of normalized modes increases with increasing l_α as $1/(\mathcal{M}_\alpha)^{1/2}$ (where $\mathcal{M}_\alpha$ is mode mass, which is defined as the ratio of energy in the mode to its surface velocity amplitude squared). Therefore the coupling coefficient, which is dominated by the value of eigenfunction near the surface (see § 3.3), also increases with l_α as $1/(\mathcal{M}_\alpha)^{1/2}$, and the nonlinear frequency shifts and line widths should both increase with l_α as $1/\mathcal{M}_\alpha$.

4. MODEL PROBLEM

In deriving our analytical formulae (eqs. [2.23] and [2.25]) we made several assumptions, the primary being that the phases of different modes are random. To check the validity of our theoretical formula we have analyzed a model problem consisting of a finite number of nonlinearly coupled oscillators. The coupling coefficients are taken to be the same for all triplets in this problem. Thus the resulting equations for mode energy and phase, using equations (2.13) and (2.14), are given by

$$\frac{d\phi_\alpha}{dt} = \omega_\alpha + \frac{6\omega_\alpha \kappa}{\sqrt{8}} \sum_{\beta,\gamma} \sqrt{\frac{E_\beta E_\gamma}{E_\alpha}} \cos \Phi \,, \tag{4.1}$$

$$\frac{dE_\alpha}{dt} = \frac{12 s_\alpha \omega_\alpha \kappa}{\sqrt{8}} \sum_{\beta,\gamma} \sqrt{E_\alpha E_\beta E_\gamma} \sin \Phi \,, \tag{4.2}$$

where Φ is again defined by

$$\Phi \equiv s_\alpha \phi_\alpha + s_\beta \phi_\beta + s_\gamma \phi_\gamma \,, \tag{4.3}$$

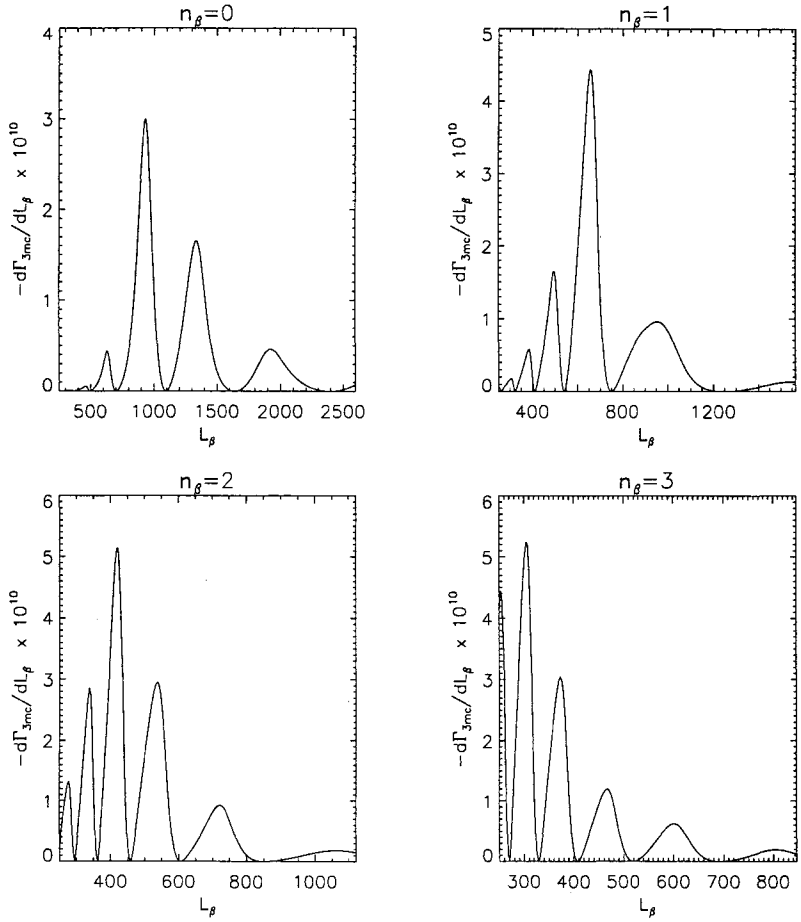

FIG. 4.—Differential contribution to nonlinear linewidth, Γ_{3mc}, as a function of l_β and n_β for a mode of frequency 3734.1 μHz. The four different panels correspond to the values of n_β increasing clockwise from 0 to 3 (top left panel is for $n_\beta = 0$). For this particular calculation we have used the boundary conditions of KG, and therefore propagating waves have continuous frequency spectrum. Moreover, the velocity power spectrum of high-degree modes ($l > 200$) has been taken to be $\propto 1/l$, and the thickness of the isothermal atmosphere is set equal to zero. The maxima in these curves occurs when the third mode lies on one of the ridges in the l-ν diagram. Note that the integrated contribution to Γ_{3mc} from a ridge (the area under the corresponding curve) is declining with increasing value of n_β. The decline is faster in the case when the velocity power spectrum is l-independent.

and κ is the coupling coefficient. We can simplify the above set of equations by using a complex mode amplitude A_α, defined to be $(E_\alpha)^{1/2} \exp(i\phi_\alpha)$, and then equations (4.1) and (4.2) compress to

$$\frac{dA_\alpha}{dt} = i\omega_\alpha A_\alpha + \frac{i6\kappa\omega_\alpha}{\sqrt{8}} \sum_{\beta,\gamma} (A_\beta + A_\beta^*)(A_\gamma + A_\gamma^*) = i\omega_\alpha A_\alpha + \frac{i3\kappa\omega_\alpha}{\sqrt{8}} \mathscr{A}^2 , \tag{4.4}$$

where

$$\mathscr{A} \equiv \sum_\beta (A_\beta + A_\beta^*) .$$

The factor of 3, instead of 6, in the last part of equation (4.4) is due to the fact that the sum over modes β and γ is over distinct doublets (the combinatorial factors in eqs. [4.1] and [4.2] require that we sum over distinct triplets). It is now easy to integrate the above set of equations numerically, and to calculate the unapproximated mode frequency shift due to nonlinear interactions. We have carried out numerical calculations with 50 modes whose frequencies lie on the f-ridge ($\omega^2 = gl/R_\odot$, where g is the gravitational acceleration at the solar surface) between l of 100 and 590 with a spacing of 10. The coupling coefficient is chosen to be 5×10^{-5}, and the mode amplitudes are set equal to unity at the initial time, so that the system is in the weakly nonlinear regime. The numerically calculated phase shifts of a selected set of modes as a function of time are shown in Figure 5. The nonlinear frequency shift calculated by the integration of the above coupled set of differential equations is found to be in reasonable agreement with equation (2.23) (see Fig. 5), thus providing credence to our analytical formula.

5. CONCLUSION

We find that the p-mode frequencies are shifted due to nonlinear interactions with other p-modes and f-modes. This shift arises primarily due to nonresonant three-mode interactions, and is dominated by high l f-modes. The largest uncertainty in our calculation is the energies of high l ($l > 500$) modes. We note however that the frequency shift scales linearly with the energies of

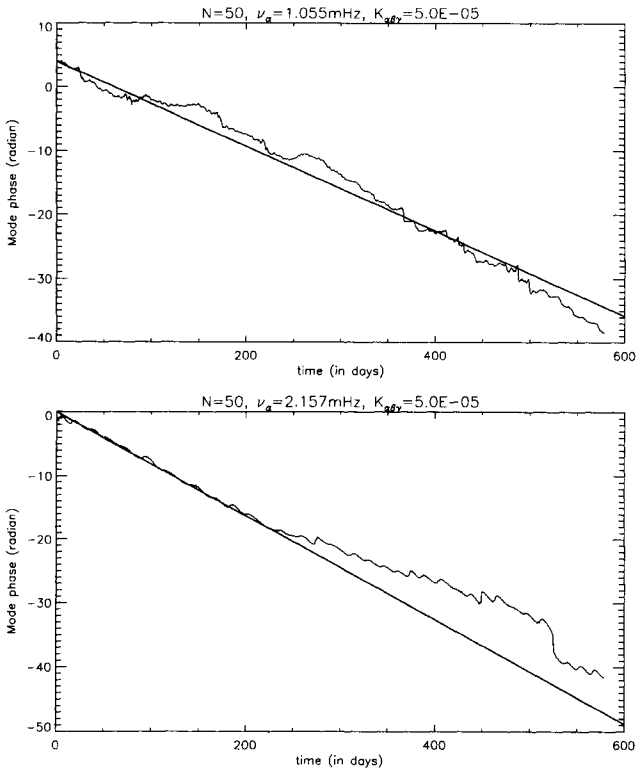

FIG. 5.—Phase as a function of time for two modes of frequencies 1.055 mHz (*top panel*) and 2.157 mHz, calculated by numerically integrating the differential equations (4.4) for the model problem. The number of modes considered here are 50, each with unit energy at time $t = 0$, and the value of coupling coefficient is chosen to be 5×10^{-5}. The slope of the thick straight line has been calculated using eq. (2.23).

these high-degree modes and therefore, it is easy to recalculate our results when mode energies are measured with more accuracy. Assuming that the mode surface velocity amplitude is independent of mode degree, we find that the magnitude of frequency shift for a radial p-mode of frequency 3 mHz is about -0.5 μHz. This is comparable to the accuracy of observed frequencies but is too small by a factor of 20–30 compared to the present day discrepancy between observed and theoretically calculated frequencies. We conclude that the nonlinear frequency shift is not of practical importance at present. However, any variation of energies of high-degree f or p modes with solar cycle will lead to a variation in nonlinear frequency shift. Thus if it turns out that mode energies vary by at least 30%–40% (we note that there is no observational evidence for such a variation at the moment) then part of the variation of p-mode frequencies with solar cycle can come from their nonlinear interaction with other modes. The nonlinear frequency shift of p and f-modes increases with l as the inverse mode mass or in other words is proportional to $l^{0.8}$. Thus, the frequency of an f-mode of $l = 1000$ is decreased, due to its interaction with other modes, by about 0.4%.

The contribution to the line width of solar radial p-modes, due to their nonlinear couplings to other modes, is found to be consistent with the earlier work of KG, and is smaller than the observed line width by a factor of at least a few.

We are grateful to Jorgen Christensen-Dalsgaard for supplying the solar model, Ken Libbrecht for the mode amplitude and line width data, and an anonymous referee for helpful comments. This research was supported in part by NSF grant AST 89-13664 and NASA grant NAGW-3018 with Caltech, and NASA grant W-17677 with HAO.

APPENDIX A

The equations of inviscid fluid dynamics for a compressible gas with internal energy $E(S, \rho)$, follow from varying the Lagrangian (Newcomb 1962)

$$L = \int d\boldsymbol{x}_0 \, \rho_0(\boldsymbol{x}_0) \left[\frac{v^2}{2} - E(S, \rho) - \psi(\boldsymbol{x}) \right]. \tag{A1}$$

The background configuration is specified by $\rho_0(\boldsymbol{x}_0)$, $p_0(\boldsymbol{x}_0)$, and $\boldsymbol{v}_0(\boldsymbol{x}_0) = 0$. The variation is achieved by displacing the position of each fluid element from $\boldsymbol{x}_0$ to $\boldsymbol{x} = \boldsymbol{x}_0 + \boldsymbol{\xi}$, where $\boldsymbol{\xi}$ is the Lagrangian displacement. Conservation of mass implies

$$\rho \, d\boldsymbol{x} = \rho_0 \, d\boldsymbol{x}_0 \Rightarrow \rho = \rho_0 \mathcal{J}^{-1}, \tag{A2}$$

where $\mathscr{J}$ is the Jacobian of the transformation. The Lagrangian can be written in terms of $\mathscr{J}$ and the background variables as

$$L = \int dx_0\, \rho_0 \left[\frac{v^2}{2} - E(S_0, \rho_0 \mathscr{J}^{-1}) - \psi(x_0 + \xi) \right], \tag{A3}$$

where $E(S_0, \rho_0 \mathscr{J}^{-1})$ is to be expanded around $E(S_0, \rho_0)$ as a series in $\rho_0(\mathscr{J}^{-1} - 1)$. The Jacobian

$$\mathscr{J} = \det\left(\frac{\partial x}{\partial x_0}\right) = \det\left(1 + \frac{\partial \xi}{\partial x_0}\right), \tag{A4}$$

may be rewritten in mixed vector and Cartesian tensor notation as

$$\mathscr{J} = 1 + (\nabla \cdot \xi) - \tfrac{1}{2}\xi^i_{;j}\,\xi^j_{;i} + \tfrac{1}{2}(\nabla \cdot \xi)^2 + \tfrac{1}{3}\xi^i_{;j}\,\xi^j_{;k}\,\xi^k_{;i} - \tfrac{1}{2}(\nabla \cdot \xi)\xi^i_{;j}\,\xi^j_{;i} + \tfrac{1}{6}(\nabla \cdot \xi)^3\,, \tag{A5}$$

where $\xi^i_{;j}$ is the covariant derivative of ξ^i with respect to x^j, and the summation convention for repeated indices is assumed. Expanding the Lagrangian in powers of the displacement, ξ, with the aid of equation (A5), we obtain the second and third-order Lagrangian densities,

$$\mathscr{L}_2 = \frac{\rho_0}{2}\left|\frac{\partial \xi}{\partial t}\right|^2 - \frac{1}{2}(\rho_0 c_0^2 - p_0)(\nabla \cdot \xi)^2 - \frac{p_0}{2}\,\xi^i_{;j}\,\xi^j_{;i} - \frac{\rho_0}{2}\,\psi_{;ij}\,\xi^i\xi^j\,, \tag{A6}$$

and

$$\mathscr{L}_3 = \frac{1}{6}\left[p_0 - \rho_0 c_0^2 + \rho_0^2\left(\frac{\partial c_0^2}{\partial p_0}\right)_S\right](\nabla \cdot \xi)^3 + \frac{1}{2}(\rho_0 c_0^2 - p_0)(\nabla \cdot \xi)\xi^i_{;j}\,\xi^j_{;i} + \frac{1}{3}\,p_0\,\xi^i_{;j}\,\xi^j_{;k}\,\xi^k_{;i} - \frac{\rho_0}{6}\,\psi_{;ijk}\,\xi^i\xi^j\xi^k\,. \tag{A7}$$

The last term in both $\mathscr{L}_2$ and $\mathscr{L}_3$ vanishes for a uniform gravitational field. The Hamiltonian and Lagrangian densities are related by

$$\mathscr{H} = \frac{\delta \mathscr{L}}{\delta \dot{\xi}^i}\,\dot{\xi}^i - \mathscr{L}\,. \tag{A8}$$

Where $\dot{\xi}^i$ represents $\partial \xi^i/\partial t$. Using equations (A6), (A7), and (A8), we derive the second- and third-order Hamiltonian densities,

$$\mathscr{H}_2 = \frac{\rho_0}{2}\left|\frac{\partial \xi}{\partial t}\right|^2 + \frac{1}{2}(\rho_0 c_0^2 - p_0)(\nabla \cdot \xi)^2 + \frac{1}{2}\,p_0\,\xi^i_{;j}\,\xi^j_{;i}\,, \tag{A9}$$

and

$$\mathscr{H}_3 = -\mathscr{L}_3\,. \tag{A10}$$

The normal mode equation is derived from $\mathscr{L}_2$ using the substitution $\xi(x, t) = \xi(x)\exp(-i\omega t)$,

$$-\rho_0 \omega^2 \xi - \nabla[(\rho_0 c_0^2 - p_0)(\nabla \cdot \xi) + \nabla \cdot (p_0 \xi)] + g\nabla \cdot (\rho_0 \xi) = 0\,. \tag{A11}$$

Writing

$$\xi = \left[\xi_r\, Y_l^m(\theta, \phi),\ \xi_h \frac{\partial Y_l^m(\theta, \phi)}{\partial \theta},\ \frac{\xi_h}{\sin\theta}\frac{\partial Y_l^m(\theta, \phi)}{\partial \phi}\right]$$

allows (A11) to be separated into

$$\frac{1}{r^2}\frac{d}{dr}(r^2\xi_r) - \frac{g}{c_0^2}\,\xi_r + \left[\frac{\omega^2}{c_0^2} - \frac{l(l+1)}{r^2}\right] r\xi_h = 0\,, \tag{A12}$$

and

$$\frac{d}{dr}(r\xi_h) + \left(\frac{N^2}{\omega^2} - 1\right)\xi_r - \frac{N^2}{g}\,r\xi_h = 0\,. \tag{A13}$$

Here N is the Brunt-Väisälä frequency given by

$$\frac{N^2}{g} = -\frac{g}{c_0^2} - \frac{d\ln\rho_0}{dr}\,.$$

The boundary conditions are that $\xi_r \to 0$ as $r \to 0$ and that the Lagrangian pressure perturbation vanishes at the outer radius of the model atmosphere.

APPENDIX B

Here we sketch the calculation of $K_{\alpha_s\beta_s\gamma_s}$. In the coordinate basis ($\boldsymbol{e}_r, \boldsymbol{e}_\theta = r\hat{\boldsymbol{e}}_\theta, \boldsymbol{e}_\phi = r\sin\theta\hat{\boldsymbol{e}}_\phi$), the eigenfunctions are as follows

$$\boldsymbol{\xi} = \left[\xi_r(r)Y_l^m, \frac{\xi_h(r)}{r}\frac{\partial Y_l^m}{\partial\theta}, \frac{\xi_h(r)}{r\sin^2\theta}\frac{\partial Y_l^m}{\partial\phi}\right]. \tag{B1}$$

The covariant derivative can be calculated using the expression

$$\xi^i_{;j} = \frac{\partial\xi^i}{\partial x^j} + \Gamma^i_{jk}\xi^k, \tag{B2}$$

where Γ^i_{jk} are the connection coefficients which are symmetric in indices j and k. The nonzero Γ^i_{jk} are given below.

$$\Gamma^r_{\theta\theta} = -r, \quad \Gamma^r_{\phi\phi} = -r\sin^2\theta, \quad \Gamma^\theta_{\phi\phi} = -\sin\theta\cos\theta,$$
$$\Gamma^\theta_{r\theta} = 1/r, \quad \Gamma^\phi_{r\phi} = 1/r, \quad \Gamma^\phi_{\theta\phi} = \cot\theta. \tag{B3}$$

With reference to equation (2.9) reproduced here

$$K_{\alpha_{s\alpha}\beta_{s\beta}\gamma_{s\gamma}} = -\frac{1}{6}\int d^3x\left\{\left[p_0 - \rho_0 c_0^2 + \rho^2\left(\frac{\partial c_0^2}{\partial\rho}\right)_S\right](\nabla\cdot\xi_{\alpha_{s\alpha}})(\nabla\cdot\xi_{\beta_{s\beta}})(\nabla\cdot\xi_{\gamma_{s\gamma}})\right.$$
$$\left. + (\rho_0 c_0^2 - p_0)[(\nabla\cdot\xi_{\alpha_{s\alpha}})\xi^i_{\beta_{s\beta};j}\xi^j_{\gamma_{s\gamma};i} + (\nabla\cdot\xi_{\beta_{s\beta}})\xi^i_{\gamma_{s\gamma};j}\xi^j_{\alpha_{s\alpha};i} + (\nabla\cdot\xi_{\gamma_{s\gamma}})\xi^i_{\alpha_{s\alpha};j}\xi^j_{\beta_{s\beta};i}] + p_0[\xi^i_{\alpha_{s\alpha};j}\xi^j_{\beta_{s\beta};k}\xi^k_{\gamma_{s\gamma};i} + \xi^i_{\beta_{sB};j}\xi^j_{\alpha_{s\alpha};k}\xi^k_{\gamma_{s\gamma};i}]\right\},$$

terms 1, 3, and 4 are trivial to reduce to a single radial integration using the following properties of spherical harmonic functions

$$\int d\Omega\left[\frac{\partial Y_{l_1}^{m_1}}{\partial\theta}\frac{\partial Y_{l_2}^{m_2}}{\partial\theta} + \frac{1}{\sin^2\theta}\frac{\partial Y_{l_1}^{m_1}}{\partial\phi}\frac{\partial Y_{l_2}^{m_2}}{\partial\phi}\right] = (-1)^{m_1}l_1(l_1+1)\delta_{l_1,l_2}\delta_{m_1,-m_2}, \tag{B4}$$

$$\int d\Omega Y_{l_1}^{m_1}Y_{l_2}^{m_2} = (-1)^{m_1}\delta l_{1,l_2}\delta_{m_1,-m_2}. \tag{B5}$$

The remaining terms are best treated by parts. Term 2 may be simplified as follows

$$I_2 = \frac{1}{6}\int d^3x\{[(\rho_0 c_0^2 - p_0)(\nabla\cdot\xi_{\alpha_{s\alpha}})]_{;r}\xi^r_{\beta_{s\beta};j}\xi^j_{\gamma_{s\gamma}} + [(\rho_0 c_0^2 - p_0)(\nabla\cdot\xi_{\alpha_{s\alpha}})]\xi^r_{\beta_{s\beta};jr}\xi^j_{\gamma_{s\gamma}}\} - \frac{1}{6}\int d\Omega r^2[(\rho_0 c_0^2 - p_0)(\nabla\cdot\xi_{\alpha_{s\alpha}})\xi^r_{\beta_{s\beta};j}\xi^j_{\gamma_{s\gamma}}]. \tag{B6}$$

Term 5 can be reduced by parts to

$$I_5 = \int d^3x p_0\{[\xi^i_{\alpha_{s\alpha};j}\xi^j_{\beta_{s\beta}}\xi^k_{\gamma_{s\gamma};i}]_{;k} - \xi^i_{\alpha_{s\alpha};jk}\xi^j_{\beta_{s\beta}}\xi^k_{\gamma_{s\gamma};i} - \xi^i_{\alpha_{s\alpha};j}\xi^j_{\beta_{s\beta}}\xi^k_{\gamma_{s\gamma};ki}\}. \tag{B7}$$

Further progress is rendered by the simple identity

$$\int d^3x\psi(r)\nabla\cdot V = \int d^3x\frac{\psi(r)}{r^2}\frac{\partial}{\partial r}(r^2V_r).$$

Term 6 is obtained from term 5 by permuting β and γ.

Angular integrations present the selection rules, which, for the case of a radial mode α, read $s_\beta m_\beta + s_\gamma m_\gamma = 0$ and $l_\beta = l_\gamma$.

APPENDIX C

We compare the relative magnitudes of four-mode and three-mode couplings in this Appendix. From equations (2.6) and (2.7) we see that each term for four-mode couplings contains an extra factor of $E^{1/2}$ (where E is mode energy), and from equation (2.9) we note that the four-mode coupling coefficient, $K_{\alpha\beta\gamma\delta}$, contains an extra $\xi^i_{;j}$ factor compared to the three-mode coupling coefficient $K_{\alpha\beta\gamma}$. Finally, the four-mode coupling phase space is larger than the three-mode coupling phase space due to the sum over an additional degree of freedom in the fourth angular momentum. We put all these factors together to estimate the ratio of four-mode to three-mode coupling results.

We saw in section 3.3 that most of the conribution to the coupling coefficient comes from near the solar surface, and that for high-degree modes the derivative of displacement eigenfunction ($\xi^i_{;j}$) is approximately equal to $l/(R_\odot\omega\mathcal{M}^{1/2})$, where ω and $\mathcal{M}$ are mode frequency and mass respectively. Thus each term in four-mode couplings will be smaller than three-mode couplings by a factor of $lE^{1/2}/(R_\odot\omega\mathcal{M}^{1/2})$.

In all three-mode interactions involving a radial mode α, modes β and γ must have the same degree. However, in the case of four-mode couplings involving the mode α, for given (l_β, m_β), the values of (l_γ, m_γ) and (l_δ, m_δ) are constrained only by the triangularity condition, and the m matching condition. Thus for each (l_β, m_β) there are roughly l_β^3 quadrupulets due to the freedom in l_γ, l_δ, and the m's, and so the phase space for four-mode couplings is larger compared to three-mode couplings by a factor of l_β^3.

However, using the result of § 3.5 we know that the part of $K^2_{\alpha\beta\gamma\delta}$ which depends on the angular integral of the product of three spherical harmonic functions will be smaller than $K^2_{\alpha\beta\gamma}$ which involves two spherical harmonic functions by a factor of l_β. Thus the four-mode phase space is effectively larger than three-mode space by a factor of l^2_β.

Combining the above results we find the ratio of four-mode to three-mode interaction to be $\sim l^4 E/(R^2_\odot \omega^2 \mathcal{M}) \sim V^2_{\rm modes}/C^2_s$, where $V_{\rm modes}$ is the velocity associated with oscillations at the surface, and C_s is the sound speed at the surface. Substituting $l \sim 2000$, $\omega \sim 0.02$, $E \sim 10^{23}$ and $\mathcal{M} \sim 10^{23}$ into this result, we find that four-mode coupling is smaller than three-mode couplings by a factor of about 10^5.

REFERENCES

Christensen-Dalsgaard, J. 1991, in Challenges to Theories of the Structure of Moderate-Mass Stars, ed. D. Gough & J. Toomre (New York: Springer-Verlag)

Dziembowski, W. 1982, Act. Astron., 32, 147

Edmonds, A. R. 1960 Angular Momentum in Quantum Mechanics (Princeton: Princeton Univ. Press)

Goldreich, P., & Kumar, P. 1990, ApJ, 363, 694

Kaufman, A. 1991, Ph.D. thesis, Caltech

Kumar, P., & Goldreich, P. 1989 ApJ, 342, 558 (KG)

Lavely, E. 1990, Ph.D. thesis, MIT

Libbrecht, K. G., & Woodward M. F. 1991 Science, 253, 152

Misner, C. W., Thorne, K. S., & Wheeler, J. A. 1973 Gravitation (San Francisco: Freeman)

Newcomb, W. A. 1962, Nuclear Fusion: Supplement Part 2 (Vienna: International Atomic Energy Agency), 451

Wentzel, D. G. 1987, ApJ, 319, 966